Reduction of Charge-Carrier Recombination at ZnO–Polymer Blend Interfaces in PTB7-Based Bulk Heterojunction Solar Cells Using Regular Device Structure: Impact of ZnO Nanoparticle Size and Surfactant

Sadok Ben Dkhil, Meriem Gaceur, Abdou Karim Diallo, Yahia Didane, Xianjie Liu, Mats Fahlman, Olivier Margeat, Jörg Ackermann, Christine Videlot-Ackermann

Reduction of charge carrier recombination at ZnO/polymer blend interface in PTB7-based bulk heterojunction solar cells using regular device structure: Impact of ZnO nanoparticle size and surfactant

Sadok Ben Dkhil,[1] Meriem Gaceur,[1] Abdou Karim Diallo,[1] Yahia Didane,[1] Xianjie Liu,[2] Mats Fahlman,[2] Olivier Margeat,[1] Jörg Ackermann[1,], Christine Videlot-Ackermann[1,]**

[1] Aix Marseille Université, UMR CNRS 7325, CINaM, Marseille, France.

[2] Department of Physics, Chemistry and Biology Linkoping University, S8183, Linkoping, Sweden.

KEYWORDS: ZnO nanoparticles; surfactant; nanodispersion; interfacial layer; polymer blend; morphology; power conversion efficiency; charge carrier recombination.

ABSTRACT: Cathode interfacial layers also called electron extraction layers (EELs) based on zinc oxide (ZnO) have been studied in polymer blend solar cells towards optimisation of the opto-electric properties. Bulk heterojunction solar cells based on poly({4,8-bis[(2-ethylhexyl)oxy]benzo[1,2-*b*:4,5-b′]dithiophene-2,6-diyl}{3-fluoro-2-[(2-ethylhexyl)carbonyl]thieno[3,4-*b*]thiophenediyl}) (PTB7) and [6,6]-Phenyl-C71-butyric acid methyl ester ($PC_{70}BM$) were realized in regular structure with all-solution-processed interlayers. Two commercially available surfactants, ethanolamine (EA) and ethylene glycol (EG), were used to modify the surface of ZnO nanoparticles (NPs) in alcohol-based dispersion. The influence of ZnO particle size was also studied by preparing dispersions of two NP diameters (6 nm *vs.* 11 nm). Here, we show that performance improvement can be obtained in polymer solar cells via use of solution-processed ZnO EELs based on surface-modified nanoparticles. By optimizing the ZnO dispersion, surfactant ratio and the resulting morphology of EELs, PTB7:$PC_{70}BM$ solar cells with power conversion efficiency of 8.2% could be obtained using small sized EG-modified ZnO NPs that allow to clearly enhance the performance of solution-processed photovoltaic devices compared to state-of-the-art ZnO based cathode layers.

1. Introduction

Polymer solar cells (PSCs) have attracted high attention as future solar cells due to proposing real advantages such as being lightweight and low-cost compared to traditional photovoltaic technologies. The efficiency of PSCs has be strongly improved over the last few years, thanks to

intensive development of new materials process photoactive layers as well as interfacial layers (IL), novel device structures were also proposed using various combination of IL materials. Thanks to insertion of functional ILs, i.e. electron extraction layer (EEL) and hole extraction layer (HEL), between the electrode and the photoactive layer, the performance of the organic solar cells could be clearly increase.[1-3] In device structures reported in recent works, the interface between the cathode and the photoactive layer plays specific roles in charge transport, extraction and collection. To be compatible with low cost PSCs processing from solution, intensive work has been dedicated to develop improved EELs compatible with solution-processing. To reach high efficiency in PSCs, EELs have to fulfill the three major requirements: (1) suitable energy level alignment between photoactive layer and the cathode to ensure an ohmic contact for electron transport and collection, (2) have efficient hole blocking properties leading to selective extraction of electrons and (3) be chemically and physically stable in order to resist degradation.

Amongst solution processed interfacial materials, metal oxides such as zinc oxide (ZnO),[4-10] titanium dioxide (TiO_2)[11-13] or hybrid reduced graphene oxide (RGO)/metal oxide nanocomposite using either ZnO or TiO_2[14] are also interesting materials with suitable energy level to extract electrons from fullerene derivatives combined with a simple synthesis, low environmental toxicity and energy impact. Use of quantum confinement of ZnO nanoparticles (NPs) allows further tune gap and energy level on the EELs.[15-17] Reduction of the energy barrier between EEL and a photoactive layer by using interfacial dipole layers related to surface modification of the metal oxide interlayers have been successfully applied to further improve the device performanc.[18] Indeed we could show that ethanolamine (EA) modification of ZnO interlayers generates fill factors up to 73 %.[10] Additionally to their charge extraction properties, metal oxide layers allow to produce so called optical spacer (OSP) effects leading to changes in

the light distribution inside solar cells.[19-22] As the dielectric constant of metal oxides such as ZnO is different from those of the polymer and the electrode, the optical spacer can improve the spatial light distribution inside the photoactive layer of the solar cells and thus optimizing photocurrent generation.

In the case of polymer blend solar cells based on poly({4,8-bis[(2-ethylhexyl)oxy]benzo[1,2-*b*:4,5-b′]dithiophene-2,6-diyl}{3-fluoro-2-[(2-ethylhexyl)carbonyl]thieno[3,4-*b*]thiophenediyl}) (PTB7) and [6,6]-Phenyl-C71-butyric acid methyl ester ($PC_{70}BM$) (see molecular structures in **Figure 1a**), we demonstrated in a former work that ZnO EELs lead to strongly improved charge carrier collection and efficiency of polymer solar cells although light absorption was not increased in the photoactive layer.[23] The improvement in performance was addressed to better hole blocking of the ZnO EEL as well as a contact resistance and charge carrier recombination reduction at the polymer blend/Al interface. The bulk heterojunction solar cells using regular structures with ILs processed only from solution are identical to this work and shown in **Figure 1b**. Importantly, the processing of very smooth and homogeneous ZnO films was found essential to produce highly efficient solar cells with high fill factors up to 66%. For this purpose, EA surface modification was used to produce ZnO NP isopropanol solution free of aggregates compared to pristine ZnO.[23] Small-molecule EA is a classical stabilization additive usually applied in metal salt solutions, because of its high activity with metals.[24,25] Such surfactants, even at low amount (0.2 vol.%) in the NCs based solution, coat the particles not only in dispersion but also in deposited layer and can consequently introduce a barrier to physical contact between the particles. It is therefore evident that, solution processing of efficient NC layers is delicate due to the simultaneous need of effective NP stabilization and high charge carrier transport.[26] The purpose of the paper is to study the different surfactants used in ZnO

dispersions to form high-efficiency EELs for regular device structures. We used two types of commercially available surfactant, *i.e.* EA and ethylene glycol (EG) (see molecular structure in **Figure 1c**), as organic molecules in alcohol-based solvent. While poly(ethylene glycol) was used previously in the literature to form ZnO/poly(ethylene glycol) hybrids as EELs,[27,28] the selection in the present study was voluntary focused on small insulating molecules to minimize steric effects. The semiconductor-insulator composite was applied as EEL in solar cells. Additionally, two ZnO nanoparticles sizes were used to prepare the solution-processable dispersions: ZnO NPs with 6 nm (ZnO-a) or 11 nm (ZnO-b) as average diameters, respectively (**Figure 1c**). The modification of electrical and morphological properties of ZnO NPs by the addition of EA or EG as surfactants were studied and discussed in details towards performance improvement of solution-processed solar cells.

2. Experimental

Inks preparation. Two ZnO NP sizes (see **Figure 1c**) were prepared following the procedures described previously.[23,29,30] In the present study, ZnO NPs with 6 nm as average diameter are named ZnO-a, while NPs with 11 nm as average diameter are named ZnO-b. The solution of ZnO NPs were prepared by transferring the as-synthesized ZnO-a or ZnO-b NPs from the reaction medium to isopropanol mixed with EA or EG to a concentration of 5 mg/mL. The molecular structure of EA and EG are shown in **Figure 1c**. The ratio of surfactant ranged from 0.2 to 1 vol.%. For instance 1 vol.% of EA represents 1 µL in 1 mL of 5 mg/mL of ZnO in isopropanol. The mixing of ZnO with surfactant in isopropanol induces optical modification of

the ZnO solution that are immediately visible once the surfactant was introduced in the solution. Ultrasonic treatment of 10 min furthermore increases the solubility of ZnO NPs. Surfactant-free ZnO dispersion was prepared as reference (pristine ZnO). Size distribution of the ZnO NCs was measured by dynamic light scattering (DLS) methods using a NanoZetaSizer from Malvern.

Solar cell fabrication and characterization. Polymer solar cells were fabricated using regular device structure as detailed in former work.[23] **Figure 1b** shows the device structure used in this work which is identical to our recently work. Importantly, we used shadow mask 0.27 cm^2 in size that are equal in size and shape to the solar cell (size of 0.27 cm^2).By comparing the performance of masked and unmasked device, we found less than 2% photocurrent increase for unmasked devices indicating that our device structure and size is suitable to avoid photocurrent overestimation.[31] J-V curves of solar cells and photovoltaic parameters are presented for best devices, while average PCEs obtained with standard deviation analysis were calculated using 6 devices.

TFT samples preparation. The as-synthesized ZnO-a or ZnO-b NPs were dissolved in isopropanol mixed with 1 vol.% of EA or 1 vol.% of EG to a constant concentration of 30 mg/mL. For lower concentrations, no charge transport could be observed.[32] The schematic representation and an optical microscopy image of the TFT architecture are shown in **Figures S1**. Device preparation is identical to former work,[33] however, in the present work no HMDS treatment was applied.[34]

Samples characterizations. ZnO NPs were characterized by the high-resolution transmission electron microscope (HR-TEM) JEOL 3010, where samples were prepared by drop casting of diluted solution on a mesh-coated carbon film. Photoluminescence (PL) and morphology

investigations of ZnO NPs based thin films where recorded using a CARY Eclipse spectrometer and a scanning electron microscope (SEM) from JEOL (JSM 6340F) after spin-coating of solutions onto glass substrates at 1500 rpm for 1 minute and dried on a hot plate at 80°C for 5 minutes. The surface morphology of ZnO NP layers deposited on top of PTB7:$PC_{70}BM$ layers was studied by atomic force microscopy (AFM) using a Nanoscope III in taping mode in air. Ultraviolet photoelectron spectroscopy (UPS) and X-ray photoelectron spectroscopy (XPS) measurements were performed in an ultrahigh vacuum (UHV) surface analysis system with a Scienta-200 hemispherical analyzer by using ZnO NP samples spin-coated onto ITO substrates with the resulting film thickness ~20 nm. UPS and XPS measurement were calibrated by referencing to Fermi level and Au $4f_{7/2}$ peak position of the Ar+ ion sputter-clean gold foil. UPS was carried out with an unfiltered HeI ($h\upsilon$ = 21.22 eV) to characterize the vacuum level and the valence states with an error margin of ±0.05 eV. The work function was derived from the secondary electron cut-off. XPS was measured with a monochromatized Al *K*α source ($h\upsilon$ = 1486.6 eV).

3. Results and discussion

The chemical structure of organic compounds involved in blend active layers and a schematic representation of the regular device structure used in the present study are shown in **Figure 1a** and **Figure 1b**, respectively. **Figure 1c** shows HR-TEM images of ZnO NPs with average diameters of 6 nm (ZnO-a) or 11 nm (ZnO-b) together with the molecular structure of surfactants, EA and EG, used to modify the surface of ZnO NPs in solution state. Modified ZnO NPs were then used to form EELs in solar cells based on PTB7:$PC_{70}BM$ blend as active layer.

Here, we emphasis the influence of surfactant and NPs size on the properties of ZnO composites and thus on performances of PTB7:$PC_{70}BM$ based solar cells.

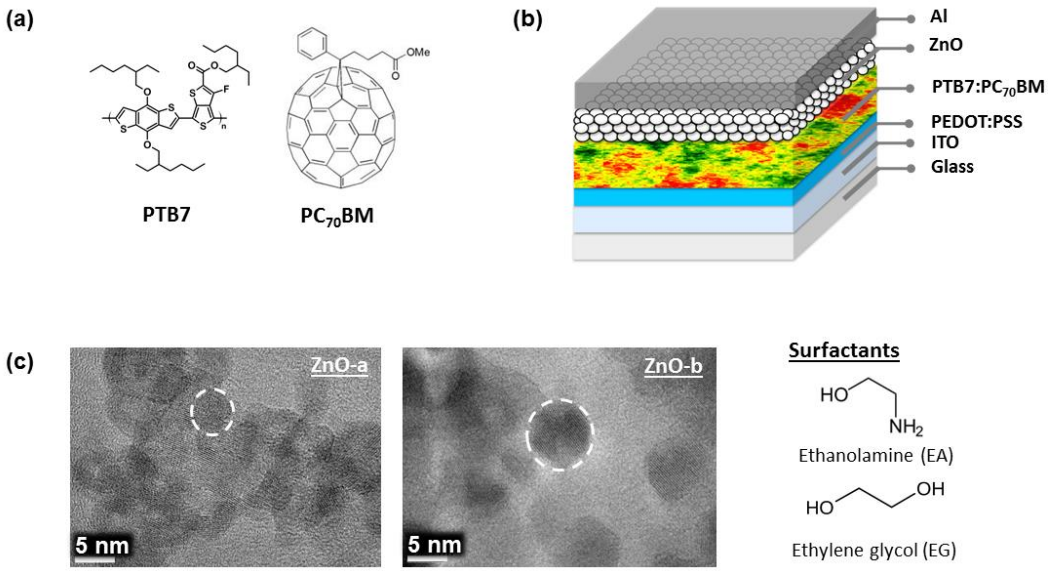

Figure 1. (a) Chemical structures of PTB7 and $PC_{70}BM$, (b) Schematic representation of device structure and (c) TEM images of ZnO-a and ZnO-b with chemical structure of surfactants.

The solution of ZnO NPs were prepared by transferring the as-synthesized ZnO-a or ZnO-b NPs from the reaction medium to isopropanol using EA or EG as surfactants. **Figure 2** shows the corresponding optical images of ZnO-a and ZnO-b dispersions in isopropanol at 5 mg/mL of ZnO with 1 vol.% of EA or EG. The pristine ZnO dispersion presents large aggregates revealed by a milky white aspect.[33] The mixing of ZnO with surfactant in isopropanol induces optical modification of the ZnO solution that are immediately visible once the surfactant was introduced in the solution. Ultrasonic treatment of 10 min furthermore increases the solubility of ZnO. As

contrary by changing the surfactant from EA to EG, introduction of 1 vol.% of EG leads to less translucent dispersions for the small ZnO-a NPs, while a still milky white aspect was reached for ZnO-b. In general, the milky aspect results from a light scattering inside the solution due to the presence of large agglomerates in solution state.[23] Therefore we can conclude that EA as surfactant reduces more efficiently the aggregation size and the number of large aggregates compared to EG, while larger NP sizes introduce persistent presence of large aggregates, but still with a lower amount in the case of EA compared to EG.

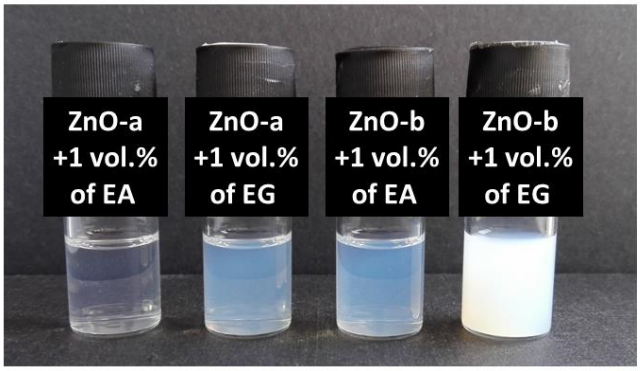

Figure 2. Optical images of solutions based on ZnO nanoparticles (ZnO-a or ZnO-b) in isopropanol at 5 mg/mL with 1 vol.% of EA or with 1 vol.% of EG.

In order to analyse the changes in aggregation size of the different ZnO solution more in details, we applied DLS as common technique to measure the mean effective hydrodynamic diameter of nanoparticles or colloids in solution. The DLS measurements were performed as a function of surfactant volume (vol.%) of EA or EG introduced into the ZnO-a and ZnO-b dispersions in isopropanol (**Figure 3**). Importantly, the concentration of ZnO was equal for all solutions at 5 mg/mL in isopropanol, the concentration used to process the EELs on top of the photoactive

layer. DLS measurements reveal that pristine ZnO-a and ZnO-b NPs in isopropanol at 5 mg/mL of ZnO form agglomerates with diameter greater than 100 nm, and thus much larger than the single particle size as obtained from HR-TEM analysis (**Figure 1c)**. By adding EA as surfactant with a ratio ranging from 0.2 to 1 vol.%, the DLS measured diameter drops to 9-10 nm and 13-14 nm for ZnO-a and ZnO-b, respectively. Such values correspond in each case to the hydrodynamic diameter of single NPs. The lower transparency of EA solution using large ZnO-b is addressed to the presence of a small amount of residual larger aggregates, which however do not impact performance of the solar cells as shown later. Remarkably, EA modified ZnO NPs in isopropanol form highly stable cluster free solution over several days independently of NPs size. On the contrary, DLS analyses reveal a different behavior depending on the size of ZnO NPs when using EG as surfactant. Any DLS experiment was possible for the dispersion based on the biggest ZnO-b NPs due to the presence of large agglomerates. For ZnO-a, the addition of EG at 0.2 vol.% does not significantly reduce the size of agglomerates compared to the pristine dispersion with a hydrodynamic diameter of 105 nm, while the aggregation size is reduced already to the single NP level for EA at this concentration. When increasing from 0.5 to 1 vol.% of EG, the DLS measurements show a major peak in the size-range of 50-66 nm even after ultra-sonic treatment. This value is 5 to 6 times higher than that obtained with EA indicating persistent agglomerates inside ZnO solutions with EG. It is thus obvious that surfactants, *i.e.* EA or EG, modify the particle surface and control their interaction in solution to form either isolated NPs or agglomerates. Although both selected surfactants are organic molecules with a small chain containing two saturated hydrocarbons, the nature of functional end-groups (amine and hydroxyl for EA or hydroxyls for EG) gives specific chemical interaction properties with the ZnO surface.

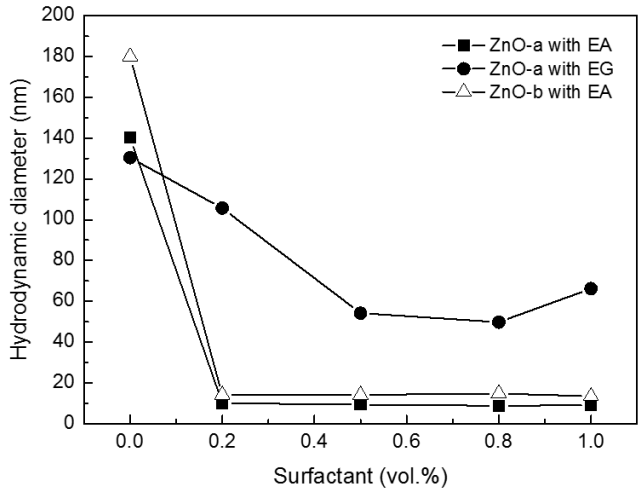

Figure 3. DLS measured-hydrodynamic size vs. the volume (vol.%) of EA or EG as surfactant in ZnO (ZnO-a and ZnO-b) dispersions at 5 mg/mL in isopropanol.

To understand the effects of EA or EG molecules on the properties of ZnO in solid state, the morphology of the different ZnO composites were investigated. **Figure 4** shows the AFM images of EA- or EG-modified ZnO (ZnO-a and ZnO-b) composite films deposited on PTB7:$PC_{70}BM$ active layers. The EG-modified ZnO composites appeared to have larger domains than EA-modified ones, respectively. A direct impact was also observed on the surface roughness. In the case of EA-modified ZnO-a composite, a root-mean-square roughness (R_{rms}) of 2-3 nm is observed while this value only slightly increases to 2.5-4 nm with EG. For ZnO-b composites, more significant changes were observed. While a well nanostructured surface was observed with EA (R_{rms} = 3-4 nm), the composite layer with EG exhibited a coarser surface with a R_{rms} to 7-10 nm resulting from the dispersion of agglomerates rather than single nanoparticles. As already observed, the large agglomerates present in solution state were partially dislocated by centrifugation during the spin-coating process making possible the deposit of thin film.[33] SEM

images (**Figure S2** and **Figure S3**) show such changes form smooth well-nanostructured layers to layers with volumic asperities *vs.* NPs size and surfactant nature. While EA molecules are grafted to ZnO to form single NPs in both solution and solid state, EG molecules capped clusters of NPs as persistent agglomerates are present in resulting solid state.[27] The inset of **Figure 4** gives a schematic representation of ZnO composites within each EG-modified composites. In order to estimate if EG also fills the surface oxygen vacancies as PEG,[35] we performed photoluminescence spectra (**Figure 5**) on the different composite films. The PL spectra show that adding EG to the solution lowers the emission intensity of the peak that corresponds to emission of shallow surface traps of ZnO. Contrary to EA chains grafted on ZnO NPs,[23] this result suggests that the EG chains interacted with the ZnO surface to passivate the shallow trap sites. While ZnO-b composites give an almost complete quenching of the defect emission, the coarser surface formed by large aggregates together with ZnO-free area in EG-modified composite will not benefit to efficient devices.[23] We suspect that the EG chains are not long enough to cap around the biggest ZnO-b NP surface to form uniform nanoclusters of suitable size as EA-grafted surfactant.

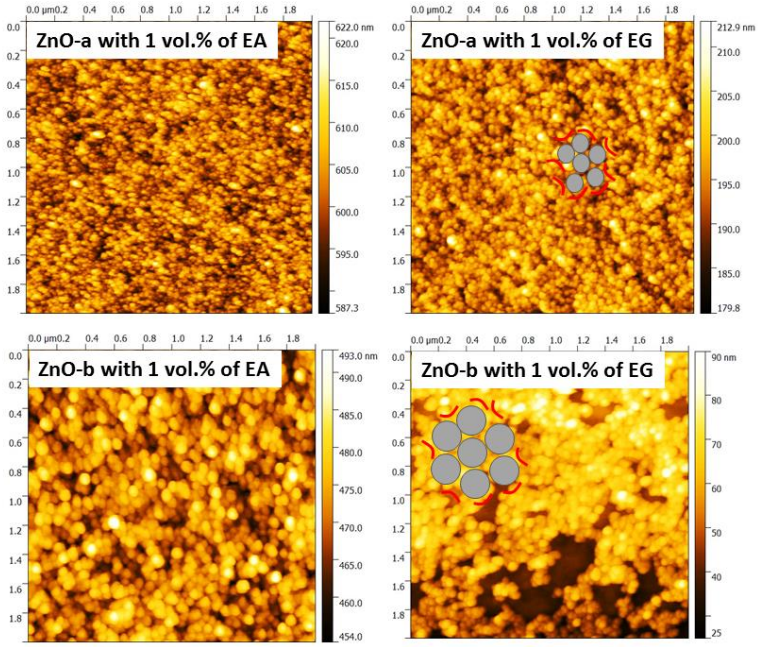

Figure 4: AFM images (2×2 μm^2) of modified-ZnO films deposited on PTB7:$PC_{70}BM$ active layers. The inset shows a schematic representation (not to scale) of ZnO-EG composite within each layer.

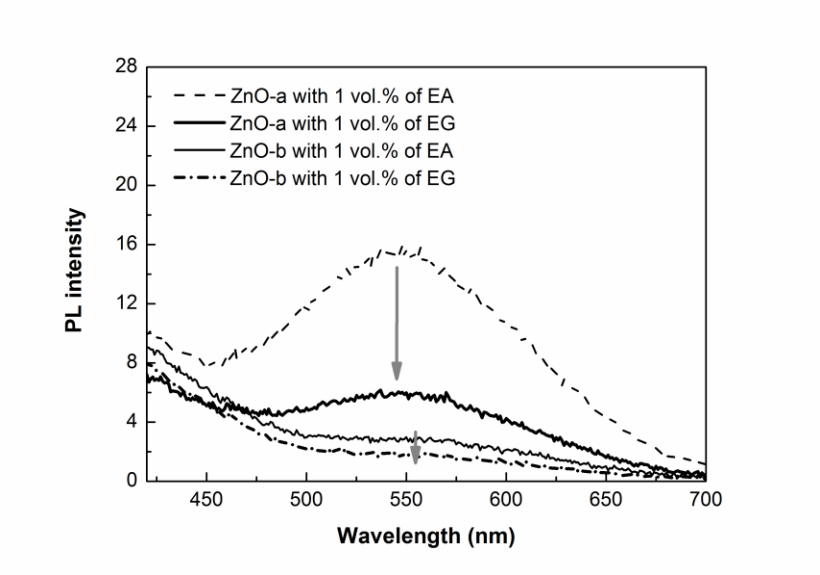

Figure 5: Emission spectra of modified-ZnO composite films deposited on glass substrates.

In order get deeper insight to modifications to the surface electronic structure induced by EA or EG, XPS and UPS measurements of thin films from both ZnO-a and ZnO-b composites were carried out. While **Figure S4** shows the entire XPS spectra, the spectra located to the O1s feature of ZnO-a and ZnO-b with EA or EG surfactants are displayed in **Figure 6**. As the surfactants will locate at the surface of the NP, the O1s spectra are expected to contain signal from EA or EG, respectively. The O1s feature of EA is located at ~532.7 eV, the same as for EG. Neat ZnO NP films typically have an asymmetric O1s core level feature with a main peak at ~531.4 eV (representing the oxygen atom in the ZnO matrix) and a shoulder at higher binding energy, ~532.9 eV (corresponding to oxygen atom vacancies and chemisorbed oxygen).[29] For EG-modified ZnO-a, the O1s spectrum retains the basic features of neat ZnO NP films, suggesting a very thin EG coverage (~monolayers), whereas the EA-modified ZnO-a NPs have a O1s spectrum dominated by the EA oxygen and the oxygen feature related to oxygen in the ZnO matrix is severely suppressed, indicating a thick EA shell. The same trends hold true for the ZnO-b NP films, but here the coverage for both the EA and EG are thinner than for the respective ZnO-a case, with e.g. the oxygen from the ZnO matrix now being visible for the EA-modified NPs. With an identical amount of surfactants (1 vol.% of EA or 1 vol.% of EG) in ZnO NP based solutions at 5 mg/mL in isopropanol, this observation may be directly related to an increased size of NPs from ZnO-a to ZnO-b. The Zn2p spectra (**Figure S5**) show no significant variation in binding energy or feature shape, but the relative intensity of the Zn features is increased for the EG-modified ZnO NPs as compared to the EA-modified NPs, indicative of thinner EG shells, and the relative trend of surfactant shell thickness between ZnO-a and ZnO-b

is followed as well. The evolution of the C1s core level also follows trend of thick EA and thin EG shells (**Figure S6**).

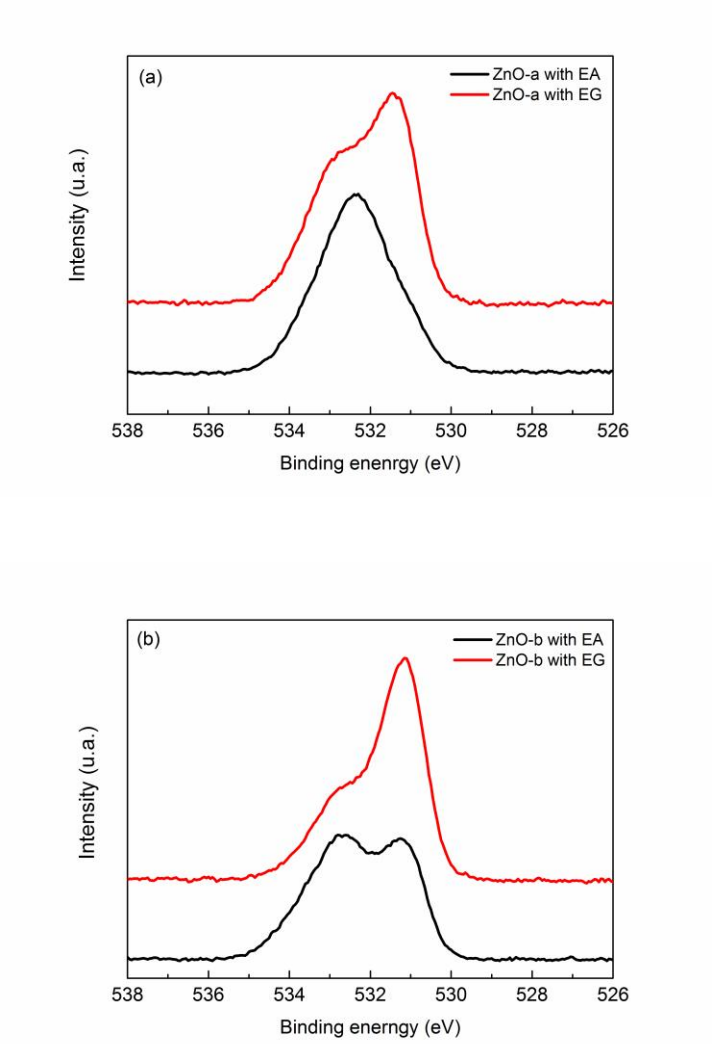

Figure 6. XPS spectra (O1s area) of ZnO-a (a) and ZnO-b (b) nanoparticles modified with surfactant (1 vol.% of EA or 1 vol.% of EG).

In **Figure 7a** (ZnO-a) and **Figure 7b** (ZnO-b), the UPS cut-off spectra (left panels) and valence band region (right panels) are shown. The work function is derived from the position of the

secondary electron cut-off, E_{co}, as WF = 21.22 – E_{co}.[36] The results show a slightly lower work function for EA-modified NPs as compared with EG-modified NPs: ~3.8 eV vs ~3.95 eV for ZnO-a and ~3.8 eV vs ~4 eV for ZnO-b NPs. This is in agreement with previous reported work, where EA treatment was found to decrease the work function compared to pristine ZnO due to dipolar polarization of the ZnO surface via the adsorption of EA.[23] The valence band edge (right panels of **Figure 7**) of the EG-modified ZnO NP films are situated closer to the Fermi energy than for the corresponding EA-modified NP films, with EG-modified ZnO-b NPs having the lowest hole injection barrier. The corresponding ionization potential (IP) values are: 8 eV and 7.6 eV for EA- modified ZnO-b NPs and EG- modified ZnO-b NPs, respectively.[36] A schematic corresponding energy level diagram of solar cells using EA- or EG-modified ZnO (ZnO-a and ZnO-b) NPs as interfacial layers is depicted in **Figure 8**. With a small variation in work function *vs* surfactant EA or EG, any films used as EELs in solar cells are expected to form pinned contacts with $PC_{70}BM$ while still blocking hole diffusion, as the valence band edges are situated deep *vs* the valence band of PTB7. Furthermore, the thinner EG shells will provide less of a tunnel barrier for the electron injection as compared to the thicker EA shells.

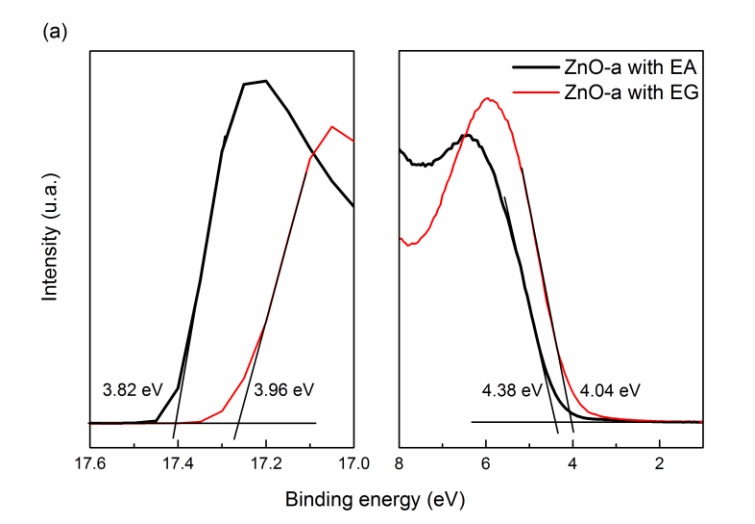

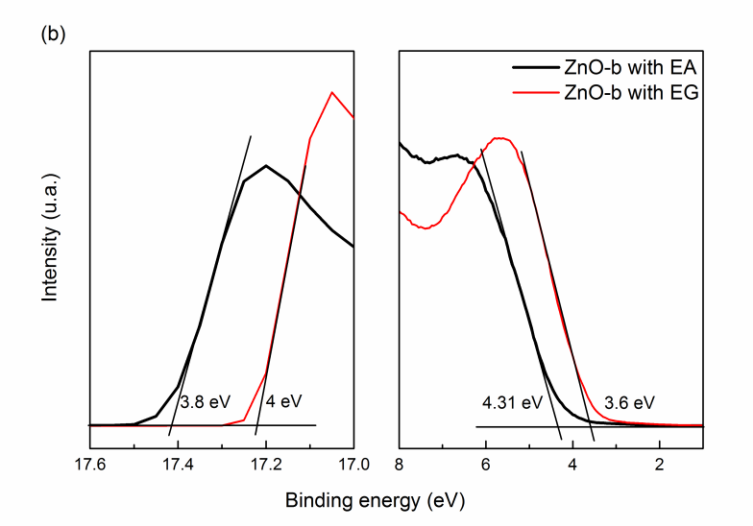

Figure 7. UPS spectra of ZnO-a (a) and ZnO-b (b) nanoparticles modified with surfactant (1 vol.% of EA or 1 vol.% of EG).

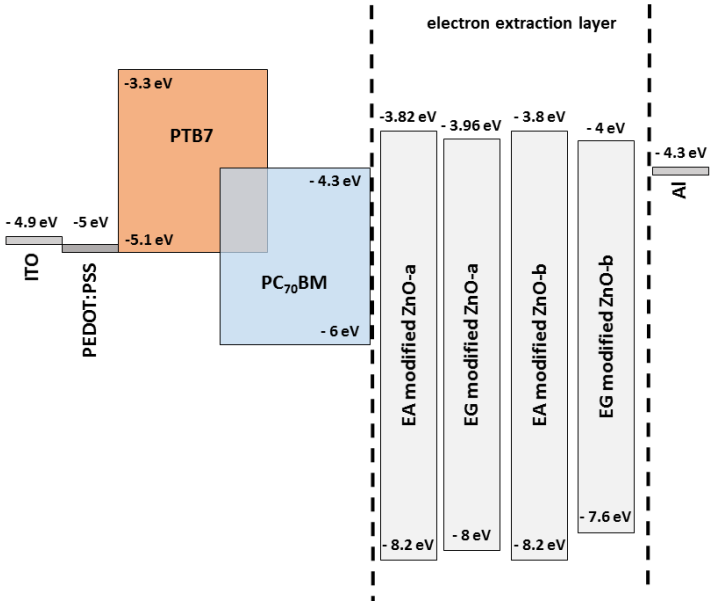

Figure 8. Energy level diagram of solar cells using EA- or EG-modified ZnO (ZnO-a and ZnO-b) electron extraction layers.

The electrical properties of modified-ZnO composites as EELs were investigated by fabricating devices with the same structure ITO/PEDOT:PSS/PTB7:$PC_{70}BM$/EELs/Al. The illuminated current-voltage (J-V) curves of PTB7:$PC_{70}BM$ solar cells using EA or EG modified ZnO-a and ZnO-b as EELs are shown on **Figure 9a** and **Figure 9b**, respectively. **Table 1** summarizes the photovoltaic parameters, as the open circuit voltage (V_{oc}), the short circuit density (J_{sc}), the fill factor (*FF*) and the power energy conversion (PCE) of the corresponding solar cells. Devices without any ZnO-based EELs were also fabricated for comparison. As can be seen in **Figure 9** and **Table 1**, independently of the surfactant additive and ZnO size, the device performances were improved as ZnO EELs were inserted between the active layer and the Al electrode. This can be addressed to the hole blocking behavior of ZnO by the reducing leakage current at the cathode related to recombination of hole and electron at Al interface together with charge carrier extraction improvement.[23] Furthermore, it can be seen that solar cells processed with ZnO-b NPs show for both surfactants clearly lower efficiencies than ZnO-a based devices. Especially in the case of EG, device performance is low. The lower performance can be addressed to the nanoscale morphology of the corresponding EELs. Indeed as shown previously, layer morphology plays an important role in the electric performance of ZnO EELs.[23] For ZnO-b NP films, larger inhomogeneity in layer thickness leads to local variation in electron density due to dependence of the electric field on the layer thickness at the interface. While ZnO-b NP films were of poor layer quality, ZnO-a NP films independently of the surface ligand form high quality layer of a smooth densely packed morphology that is favorable for improved charge extraction. Comparing the performance of the corresponding solar cells, ZnO-a NPs using EG as surfactant lead to clearly improved photocurrent densities and FF compared to EA processed EELs. The

maximum efficiency was obtained with the incorporation of 1 vol.% of EG with a J_{sc} of 16.17 mA cm^{-2}, a V_{oc} of 747 mV, a FF of 68.5 % leading to an optimum power conversion efficiency of 8.27 %. While the same trend is followed, lowest photovoltaic parameters were obtained by decreasing the spin-coating speed of ZnO solutions on PTB7:$PC_{70}BM$ active layer from 2000 rpm to 1500 rpm (**Table S1**). There is thus an important influence of the surfactant on the photovoltaic parameters of the solar cells. In order to understand the improvement in FF, one has to consider that this parameter is in general limited by the competition between recombination and extraction of free charges inside the solar cell which in terms depends on the internal field and the ratio of the carrier mobilities.[37,38] These parameters determine the serial and shunt resistances across the whole devices.[39] The analysis of serial and shunt resistances of the solar cells reveals two major effects of the intercalation of EG-modified ZnO-a as EELs. The shunt resistance was clearly improved to R_{sh} = 1500 **Ω**.cm^2 while the serial resistance (R_s) was reduced compared to reference (without ZnO) and EA-modified ZnO-a films containing cells. Concerning the charge transporting layer of the EELs (**Table S2**), the mobility values of ZnO-a and ZnO-b NP films modified with EG are higher leading to a faster electron extraction towards the electrode, a reduction of serial resistance and thus less recombination at the blend layer. Furthermore we showed that EG reduces strongly the amount of defect states at the ZnO surface, while EA surfactant does not passivate the ZnO defects. We address therefore the higher shunt resistance to the passivation effect of EG leading to a reduction of deep trap sites at the interface between the polymer blend and the ZnO layer and thus lower interface recombination. As previously observed, the improved J_{sc} with EG-modified ZnO-a can be addressed to pure electrical effect.[23] Indeed the optical calculations performed on PTB7:$PC_{70}BM$ solar cells, using an intercalated ZnO layer between the cathode and the polymer blend, indicate that the number

of absorbed photons in the active layer was not modified in the case of a 90 nm thick PTB7:$PC_{70}BM$ layer in combination with a 20 nm thick ZnO layer. Additionally, the external quantum efficiency (EQE) measurements of PTB7:$PC_{70}BM$ solar cells using ZnO-a EELs processed with EA and EG (**Figure S7**) reveal that the intercalation of an EG-modified ZnO-a layer increases device performance as the EQE spectrum is enhanced over the whole absorption spectrum of the polymer blend. We attribute therefore the improvement in Jsc not to OSP effects but to optimized electrical properties of EG-modified ZnO-a due to mainly to the reduction of hole-electron recombination at the interface between polymer blend and EEL. Thus the surface modification of ZnO NPs by EG is a promising route towards further increase in efficiency of solar cells using regular device structures. It was shown that polymer solar cells using inorganic hole blocking layers in inverted device structures show generally higher power conversion efficiencies due to the formation of more favorable bulk heterojunction morphology.[40] Therefore future studies will focus on the use of different surfactants such as EA and EG in ZnO solutions in inverted device structures to potentially improve nanoscale morphology of the bulk heterojunction as well as the electrical properties of the interface between the EEL and the photoactive layer.

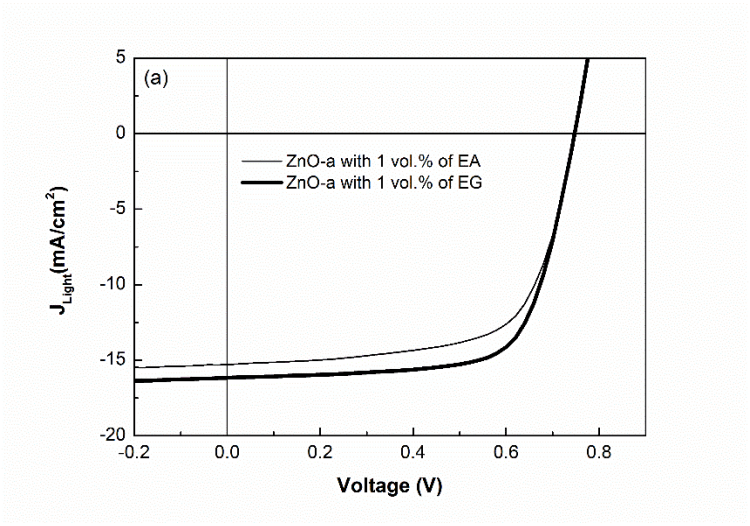

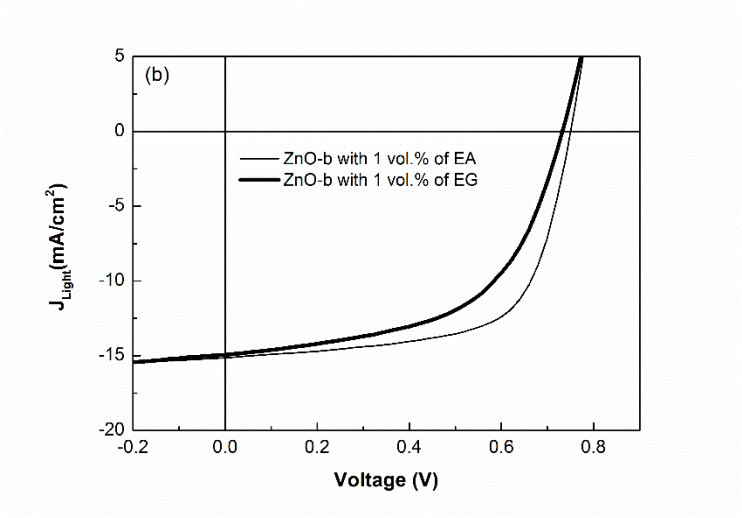

Figure 9. J-V curves under illumination of PTB7:$PC_{70}BM$ cells using ZnO-a (a) and ZnO-b (b) composites as EEL.

Table 1. Photovoltaic parameters of PTB7:$PC_{70}BM$ solar cells using EA- or EG-modified ZnO-a and ZnO-b interfacial layers. PTB7:$PC_{70}BM$ solar cell using a bare Al contact is shown as reference (w/o ZnO). Thickness of EA- or EG-modified ZnO-a and ZnO-b nanoparticle films is 20 (±2) nm.

ZnO	Surfactant	V_{oc} (mV)	J_{sc} (mA/cm^2)	FF (%)	PCE (%)	Average PCE (std dev.)	R_{sh} ($\Omega.cm^2$)	R_s ($\Omega.cm^2$)
w/o ZnO		662	14.17	61	5.72	5.33±0.33	1035	6.3
ZnO-a	EA	754	15.66	66	7.8	7.53±0.18	1250	5.5
	EG	747	16.17	68.5	8.27	7.98±0.21	1500	5
ZnO-b	EA	750	15.21	66	7.52	7.30±0.17	1150	6.5
	EG	737	14.93	55	6.06	5.81±0.2	800	12

4. Conclusion

In summary, high-efficiency organic solar cells using regular device structures based on PTB7:$PC_{70}BM$ bulk heterojunction were fabricated using solution-processed ZnO NPs modified with EA or EG as multifunctional insertion layer. The results showed that EG on smallest ZnO NPs (diameter of 6 nm) could formed a well-dispersed solutions, effectively passivated the surface traps of ZnO and lead to a faster electron extraction towards the electrode in solid state. Meanwhile, it revealed that molecular structure of the surfactant and its chemical interaction with the ZnO surface (grafting or capping) play an important role in the structural and electronic properties of

ZnO EELs. As a result, the device with EG-modified ZnO NPs exhibited the best performance. Due to an effective reduction of charge carrier recombination at ZnO-polymer blend interface, the photovoltaic performance was significantly enhanced with a maximum PCE of 8.2 % and a FF of 68.5.

Supporting Information. Device structure of ZnO-based transistors. SEM images of spin-coated ZnO thin films. XPS spectra of ZnO nanoparticles modified with surfactants. Description and data of TFT measurements. Supplementary data in solar cell characterization.

AUTHOR INFORMATION

Corresponding Authors

* *E-mail address*: videlot@cinam.univ-mrs.fr (C. Videlot-Ackermann) *and* ackermann@cinam.univ-mrs.fr (J. Ackermann)

Author Contributions

The manuscript was written through contributions of all authors. All authors have given approval to the final version of the manuscript.

ACKNOWLEDGMENT

We acknowledge financial support by the French *Fond Unique Interministériel* (FUI) under the project “SFUMATO” (Grant number: F1110019V/201308815) as well as by the European Commission under the Project “SUNFLOWER” (FP7-ICT-2011-7, Grant number: 287594). MF and XL acknowledge support from the Swedish Research Council project grant 2016-05498 and the Swedish Government Strategic Research Area in Materials Science on Functional Materials at Linköping University (Faculty Grant SFO Mat LiU No 2009 00971).

REFERENCES

(1) Wu, Z.; Song, T.; Xia, Z.; Wei, H.; Sun, B. Enhanced Performance of Polymer Solar Cell with ZnO Nanoparticle Electron Transporting Layer Passivated by in Situ Cross-Linked Three-Dimensional Polymer Network. Nanotechnology 2013, 24, 484012.

(2) Yoon, S. M.; Lou, S. J.; Loser, S.; Smith, J.; Chen, L. X.; Facchetti, A.; Marks, T. Fluorinated Copper Phthalocyanine Nanowires for Enhancing Interfacial Electron Transport in Organic Solar Cells. Nano Lett. 2012, 12, 6315-6321.

(3) Lu, L.; Zheng, T.; Wu, Q.; Schneider, A. M.; Zhao, D.; Yu, L. Recent Advances in Bulk Heterojunction Polymer Solar Cells. Chem. Rev. 2015, 115, 12666-12731.

(4) Shao, S.; Zheng, K.; Pullerits, T.; Zhang, F. Enhanced Performance of Inverted Polymer Solar Cells by Using Poly(ethylene oxide)-Modified ZnO as an Electron Transport Layer. ACS Appl. Mater. Interfaces 2013, 5, 380-385.

(5) Boix, P.P.; Ajuria, J.; Etxebarria, I.; Pacios, R.; Garcia-Belmonte, G.; Bisquert, J. Role of ZnO Electron-Selective Layers in Regular and Inverted Bulk Heterojunction Solar Cells. J. Phys. Chem. Lett. 2011, 2, 407-411.

(6) Wilken, S.; Scheunemann, D.; Wilkens, V.; Parisi, J.; Borchert, H. Improvement of ITO-Free Inverted Polymer-Based Solar Cells by Using Colloidal Zinc Oxide Nanocrystals as Electron-Selective Buffer Layer. Org. Elec. 2012, 13, 2386-2394.

(7) Hau, S. K.; Yip, H.-L.; Baek, N. S.; Zou, J.; O'Malley, K.; Jen, A. K.-Y. Air-Stable Inverted Flexible Polymer Solar Cells Using Zinc Oxide Nanoparticles as an Electron Selective Layer. Appl. Phys. Lett. 2008, 92, 253301.

(8) Liang, Z.; Zhang, Q.; Wiranwetchayan, O.; Xi, J.; Yang, Z.; Park, K.; Li, C.; Cao, G. Effects of the Morphology of a ZnO Buffer Layer on the Photovoltaic Performance of Inverted Polymer Solar Cells. Adv. Funct. Mater. 2012, 22, 2194-2201.

(9) Tan, M. J.; Zhong, S.; Li, J.; Chen, Z.; Chen, W. Air-Stable Efficient Inverted Polymer Solar Cells Using Solution-Processed Nanocrystalline ZnO Interfacial Layer. ACS Appl. Mater. Interfaces 2013, 5, 4696-4701.

(10) Lee, B. R.; Jung, E. D.; Nam, Y. S.; Jung, M.; Park, J. S.; Lee, S.; Choi, H.; Ko S.-J.; Shin, N. R.; Kim, Y.-K.; Kim, S. O.; Kim, J. Y.; Shin, H.-J.; Cho, S.; Song, M. H. Amine-Based Polar Solvent Treatment for Highly Efficient Inverted Polymer Solar Cells. Adv. Mater. 2014, 26, 494-500.

(11) Hayakawa, A.; Yoshikawa, O.; Fujieda, T.; Uehara, K.; Yoshikawa, S. High Performance Polythiophene/Fullerene Bulk-Heterojunction Solar Cell with a TiOx Hole Blocking Layer. Appl. Phys. Lett. 2007, 90, 163517.

(12) You, J.; Chen, C.-C.; Dou, L.; Murase, S.; Duan, H.-S.; Hawks, S. A.; Xu, T.; Son, H. J.; Yu, L.; Li, G.; Yang, Y. Metal Oxide Nanoparticles as an Electron-Transport Layer in High-Performance and Stable Inverted Polymer Solar Cells. Adv. Mater. 2012, 24, 5267-5272.

(13) Steim, R.; Choulis, S. A.; Schilinsky, P.; Brabec, C. J. Interface Modification for Highly Efficient Organic Photovoltaics. Appl. Phys. Lett. 2008, 92, 093303.

(14) Jayawardena, K. D. G. I.; Rhodes, R.; Gandhi, K. K.; Prabhath, M. R. R.; Dabera, G. D. M. R.; Beliatis, M. J.; Rozanski, L. J.; Henley, S. J.; Silva, S. R. P. Solution Processed Reduced Graphene Oxide/Metal Oxide Hybrid Electron Transport Layers for Highly Efficient Polymer Solar Cells. J. Mater. Chem. A 2013, 1, 9922-9927.

(15) Roest, A .L.; Kelly, J. J.; Vammaekelbergh, D.; Meulenkamp, E. A. Staircase in the Electron Mobility of a ZnO Quantum Dot Assembly due to Shell Filling. Phys. Rev. Lett. 2002, 89, 036801.

(16) Sun, B.; Sirringhaus, H. Solution-Processed Zinc Oxide Field-Effect Transistors Based on Self-Assembly of Colloidal Nanorods. Nano Lett. 2005, 5, 2408-2413.

(17) Yip, H.-L.; Hau, S. K.; Baek, N. S.; Ma, H.; Jen, A. K. Y. Polymer Solar Cells That Use Self-Assembled-Monolayer- Modified ZnO/Metals as Cathodes. Adv. Mater. 2008, 20, 2376-2382.

(18) Ma, H.; Yip, H. L.; Huang, F.; Jen, A. K. Y. Interface Engineering for Organic Electronics. Adv. Funct. Mater. 2010, 20, 1371-1388.

(19) Gilot, J.; Barbu, I.; Wienk, M. M.; Janssen, R. A. J. The Use of ZnO as Optical Spacer in Polymer Solar Cells: Theoretical and Experimental Study. Appl. Phys. Lett. 2007, 91, 113520.

(20) Roy, A.; Park, S. H.; Cowan, S.; Tong, M. H.; Cho, S.; Lee, K.; Heeger, A. J. Titanium Suboxide as an Optical Spacer in Polymer Solar Cells. Appl. Phys. Lett. 2009, 95, 013302.

(21) Jin, B.; Kim, Y.; Kim, S. H.; Lee, H.; Lee, K.; Ma, W.; Gong, X.; Heeger, A. J. New Architecture for High-Efficiency Polymer Photovoltaic Cells Using Solution-Based Titanium Oxide as an Optical Spacer. Adv. Mater. 2006, 18, 572-576.

(22) Andersen, P. D.; Skårhøj, J. C.; Andreasen, J. W.; Krebs, F. C. Investigation of Optical Spacer Layers from Solution Based Precursors for Polymer Solar Cells Using X-ray Reflectometry. Opt. Mater. 2009, 31, 1007-1012.

(23) Ben Dkhil, S.; Duché, D.; Gaceur, M.; Thakur, A. K.; Bencheikh Aboura, F.; Escoubas, L.; Simon, J.-J.; Guerrero, A.; Bisquert, J.; Garcia-Belmonte, G.; Bao Q.; Fahlman, M.; Videlot-Ackermann, C.; Margeat, O.; Ackermann, J. Interplay of Optical, Morphological and Electronic Effects of ZnO Optical Spacers in Highly Efficient Polymer Solar Cells. Adv. Energ. Mat. 2014, 1400805.

(24) Znaidi, L. Sol–gel-Deposited ZnO Thin Films: a Review. Mat. Sci. Eng. B 2010, 174, 18-30.

(25) Song, K.; Jung, Y.; Kim, Y.; Hwang, J. K.; Sung, M. M.; Moon, J. Solution-Processable Tin-Doped Indium Oxide with a Versatile Patternability for Transparent Oxide Thin Film Transistors. J. Mater. Chem. 2011, 21, 14646-14654.

(26) Kim, J.-Y.; Kotov, N. A. Charge Transport Dilemma of Solution-Processed Nanomaterials. Chem. Mater. 2014, 26, 134-152.

(27) Jo, S. B.; Lee, J. H.; Sim, M.; Kim, M.; Park, J. H.; Suk Choi, Y.; Kim, Y.; Ihn, S.-G.; Cho, K. High Performance Organic Photovoltaic Cells Using Polymer-Hybridized ZnO Nanocrystals as a Cathode Interlayer. Adv. Energy Mater. 2011, 1, 690-698.

(28) Hu, T.; Li, F.; Yuan, K.; Chen, Y. Efficiency and Air-Stability Improvement of Flexible Inverted Polymer Solar Cells Using ZnO/Poly(ethylene glycol) Hybrids as Cathode Buffer Layers. ACS Appl. Mater. Interfaces 2013, 5, 5763-5770.

(29) Bao, Q.; Liu, X.; Xia, Y.; Gao, F.; Kauffmann, L.-D.; Margeat, O.; Ackermann, J.; Fahlman, M. Effects of Ultraviolet Soaking on Surface Electronic Structure of Solution Processed ZnO Nanoparticle Film in Polymer Solar Cells. J. Mater. Chem. A 2014, 2, 17676-17682.

(30) Gaceur, M.; Ben Dkhil, S.; Duché, D.; Bencheikh, F.; Simon, J.-J.; Escoubas, L.; Mansour, M.; Guerrero, A.; Garcia-Belmonte, G.; Liu, X.; Fahlman, M.; Dachraoui, W.; Diallo, A. K.; Videlot-Ackermann, C.; Margeat, O.; Ackermann, J. Ligand-Free Synthesis of Aluminum-Doped Zinc Oxide Nanocrystals and Their Use as Optical Spacers in Color Tuned High-Efficient Organic Solar Cells. Adv. Funct. Mater. 2016, 26, 243-253.

(31) Shrotriya, V.; Li, G.; Yao, Y.; Moriarty, T.; Emery, K.; Yang, Y. Accurate Measurement and Characterization of Organic Solar Cells. Adv. Funct. Mater. 2006, 16, 2016-2023.

(32) Diallo, A. K.; Gaceur, M.; Margeat, O.; Ackermann, J.; Videlot-Ackermann, C. Towards Solution-Processed Ambipolar Hybrid Thin-Film Transistors Based on ZnO Nanoparticles and P3HT Polymer. Superlattices Microstruct. 2013, 58, 144-153.

(33) Diallo, A. K.; Gaceur, M.; Ben Dkhil, S.; Didane, Y.; Margeat, O.; Ackermann, J.; Videlot-Ackermann, C. Impact of Surfactants Covering ZnO Nanoparticles on Solution-Processed Field-Effect Transistors: From Dispersion State to Solid State. Colloids Surf., A 2016, 500, 214-221.

(34) Diallo, A.K.; Gaceur, M.; Fall, S.; Didane, Y.; Ben Dkhil, S.; Margeat, O.; Ackermann, J.; Videlot-Ackermann, C. Insight about Electrical Properties of Low-Temperature Solution-Processed Al-Doped ZnO Nanoparticle Based Layers for TFT Applications. Mater. Sci. Eng. B 2016, 214, 11-18.

(35) Sui, X. M.; Shao, C. L.; Liu, Y.C. Photoluminescence of Polyethylene Oxide-ZnO Composite Electrospun Fibers. Polymer 2007, 48, 1459-1463.

(36) Braun, S.; Salaneck, W. R.; Fahlman, M. Energy-Level Alignment at Organic/Metal and Organic/Organic Interfaces. Adv. Mater. 2009, 21, 1450-1472.

(37) Bartesaghi, D.; del Carmen Pérez, I.; Kniepert, J.; Roland, S.; Turbiez, M.; Neher, D.; Koster, L.J.A. Competition Between Recombination and Extraction of Free Charges Determines the Fill Factor of Organic Solar Cells. Nat. Commun. 2015, 6, 7083.

(38) Zhang, F.; Ceder, M.; Inganas, O. Enhancing the Photovoltage of Polymer Solar Cells by Using a Modified Cathode. Adv. Mater. 2007, 19, 1835-1838.

(39) Moliton, A.; Nunzi, J.-M. How to Model the Behaviour of Organic Photovoltaic Cells. Polym. Int. 2006, 55, 583-600.

(40) Xang, W.; Pröller, S.; Niedermeier, M.A.; Körstgens, V.; Philipp, M.; Su, B.; Moseguí González, D.; Yu, S.; Roth, S.V.; Müller-Buschbaum, P. Development of the Morphology During Functional Stack Build-up of P3HT:PCBM Bulk Heterojunction Solar Cells with Inverted Geometry. ACS Appl. Mater. Interfaces 2015, 7, 602-610.

Table of Contents